Kadirli Uygulamalı Bilimler Fakültesi Dergisi
Cilt 4, Sayı 1, 179-195, 2024

Journal of Kadirli Faculty of Applied Sciences
Volume 4, Issue 1, 179-195, 2024

Kadirli Uygulamalı Bilimler Fakültesi Dergisi

Journal of Kadirli Faculty of Applied Sciences

Numerical Study of Hydrodynamic and Thermal Characteristics in a Rectangular Grooved Duct with Circular Obstacles at Different Positions

Selma AKÇAY[1*]

[1]Çankırı Karatekin University, Engineering Faculty, Department of Mechanical Engineering, Çankırı

[1]https://orcid.org/0000-0003-2654-0702
*Corresponding author: selmaakcay@karatekin.edu.tr

Research Article

Article History:
Received: 16.09.2023
Accepted: 17.11.2023
Available online:08.03.2024

Keywords:
Rectangular grooved duct
Circular obstacles
Heat transfer
Turbulent flow
Friction factor

ABSTRACT

This study numerically evaluated the impact of the positions of circular obstacles on hydraulic and thermal characteristics in a rectangular grooved channel. Numerical study was solved by the ANSYS Fluent solver. In the study, circular obstacles were placed in the rectangular grooved channel in three different positions (Case 1, Case 2, and Case 3), and the findings were compared to the grooved duct without circular obstacles (Case 0). The walls of the grooved duct were kept at 350 K. The working fluid is air. The study was conducted for different Reynolds numbers ($2000 \leq Re \leq 10000$). The numerical findings were validated with previous study results. The simulation results indicated that the velocity and thermal fields were significantly affected by Reynolds number, position of the circular obstacles, and the geometry of the channel. According to the results, while less pressure drop occurred at the Case 3, the highest pressure drop and heat transfer were obtained at the Case 1. Convection heat transfer improved 1.78 times at Case1 and Re=10000 compared to the Case 0. For all the flow cases, the Nusselt number and the pressure loss increased with the Reynolds number. Thermo-hydraulic performance values decreased with Reynolds number due to the increase in friction factor.

Farklı Pozisyonlarda Dairesel Engellere Sahip Dikdörtgen Oluklu Bir Kanalda Hidrodinamik ve Termal Karakteristiklerin Sayısal Çalışması

Araştırma Makalesi

Makale Tarihçesi:
Geliş tarihi: 16.09.2023
Kabul tarihi: 17.11.2023
Online Yayınlanma: 08.03.2024

Anahtar kelimeler:
Dikdörtgen oluklu kanal
Dairesel engeller
Isı transferi
Türbülanslı akış
Sürtünme faktörü

ÖZ

Bu çalışma, dikdörtgen oluklu bir kanalda hidrolik ve termal karakteristikler üzerinde dairesel engellerin pozisyonlarının etkisini sayısal olarak değerlendirdi. Sayısal çalışma, ANSYS Fluent çözücü ile çözüldü. Çalışmada, dairesel engeller, dikdörtgen oluklu kanala üç farklı pozisyonda (Durum 1, Durum 2 ve Durum 3) yerleştirildi ve bulgular dairesel engellerin olmadığı oluklu kanal (Durum 0) ile karşılaştırıldı. Oluklu kanalın duvarları 350 K'de korundu. İş yapan akışkan havadır. Çalışma farklı Reynolds sayıları için gerçekleştirildi ($2000 \leq Re \leq 10000$). Sayısal bulgular önceki çalışma sonuçları ile doğrulandı. Simulsayon sonuçları, hız ve sıcaklık alanlarının kanal geometrisinden, dairesel engellerin pozisyonundan ve Reynolds sayısından önemli derecede etkilendiğini göstermiştir. Sonuçlara göre, en az basınç düşüşü Durum 3'de meydana gelirken, en yüksek basınç düşüşü ve ısı transferi Durum 1'de elde edilmiştir. Taşınımla ısı transferi, Re=10000 ve Durum 1'de Durum 0'a göre 1,78 kat iyileşmiştir. Tüm akış durumları için, Reynolds sayısı ile Nusselt sayısı ve basınç düşüşü artmıştır. Artan sürtünme faktörü nedeniyle Reynolds sayısı ile termo-hidrolik performans değerleri düşmüştür.

To Cite: Akçay S., 2024. Numerical study of hydrodynamic and thermal characteristics in a rectangular grooved duct with circular obstacles at different positions. Kadirli Uygulamalı Bilimler Fakültesi Dergisi, 4(1): 179-195.

Introduction

Wavy and grooved channels have been widely used in many engineering applications in recent years. These channels have more heat transfer surface area than straight channels. Therefore, higher thermal improvement is achieved by increasing the heat transfer area. It is preferred in many heating and cooling applications, especially in heat exchangers (Ajarostaghi et al. 2022). Many researchers examined the thermal and hydraulic behavior of wavy/grooved ducts with different geometries in experimental and numerical studies. The results of the works indicated that grooved/wavy channels provide higher thermal performance than straight channels. However, it was observed an increase in pressure drop in these channels (Kurtulmuş and Şahin 2019; Krishnan et al. 2021; Nfawa et al. 2021; Zontul et al. 2021; Alfellag et al. 2022).

Zhang and Che (2011) examined pressure drop and thermal characteristics in five different grooved ducts (elliptical, sinusoidal, trapezoidal, rectangular, and triangular) and declared that trapezoidal groove profile provided higher thermal performance and pressure drop than other channels. In their three different studies, Akdag et al. evaluated the thermal improvement under pulsating flow in sinusoidal wavy (2014), trapezoidal wavy (2016), and triangular wavy (2019) channels, and reported that heat transfer enhanced in wavy ducts with an increasing friction factor. In numerical work, Ahmet et al. (2014) examined the thermal behaviors in corrugated channels with different waveforms (sinusoidal, trapezoidal, and triangular). Their results noticed that the trapezoidal wave profile provided the highest thermal enhancement and friction factor. The results of Salami et al. (2019) indicated that the maximum Nusselt number was found in the trapezoidal corrugated duct, while the highest hydro-thermal performance was provided in the sinusoidal wavy duct. Ameur and Sahel (2019) reported that the Nusselt number increased but the friction factor decreased in rectangular, triangular, and semicircular wavy channels, respectively. Shahsavar et al. (2021) examined hydrodynamic and thermal characteristics of nanofluid flow in different waveforms (triangular, sinusoidal, and trapezoidal), and declared that heat transfer in the sinusoidal wave profile improved more than other ducts. Togun et al. (2022) executed a numerical work examining convective heat transfer of hybrid nanofluid flow in a circular corrugated duct for varying modifications of ribs at $10000 \leq Re \leq 25000$. They indicated that Nusselt number in the corrugated duct increased with Reynolds number.

Use of grooved/wavy duct to improve thermal performance is restricted. High heat transfer enhancement can be provided by using extended surfaces/obstacles and corrugated ducts together. For that reason, baffles or obstacles in different configurations are attached to corrugated ducts. The use of these modifications increases thermal performance. However, they will increase pumping power due to obstruction of flow in the duct. The effects of the obstacles inserted into the duct have been examined by many researchers. The study results indicated that the obstacles provide important improvement in heat transfer with an increasing pressure loss (Bensaci et al. 2020; Akcay, 2022; Li et al. 2022; Inan et al. 2023). In the numerical work, Handoyo and Ichsani (2016) studied impacts of delta-type obstacles on thermal improvement and flow structure in V-type wavy ducts. They examined four different ratios of obstacles (S/H: 0.5, 1, 1.5, 2). They reported that in the presence of obstacles, heat transfer can be enhanced more than 3 times compared to the without obstacles situation. Selimefendigil and Öztop (2016)'s numerical study indicated that heat transfer increase of 6.66% for the diamond-type obstacle compared to the corrugated duct without obstacles. Feng et al. (2022) investigated thermal performance of the triangular corrugated duct with trapezoidal baffles in different arrangements. They found that the friction factor and Nusselt number increased by 3.5 times and 1.7 times, respectively. The performance factor increased by 30% with the baffles. In a numerical work, Akcay and Akdag (2023) examined the impacts of the inclined baffles on thermal enhancement in a straight duct. Akcay (2023a) numerically investigated convective heat transfer for different flow velocities in a semicircular shaped grooved duct with vertical baffles. It was reported that convective heat transfer and flow structure were highly influenced by duct geometry and baffles. In another numerical study, Akcay (2023b) investigated the thermal and hydraulic behavior in a zigzag duct with winglets and declared that thermal enhancement significantly increased with the increase in friction factor in zigzag wavy channel with winglets.

As can be seen from the above works, the wavy/grooved channels greatly improve thermal performance with an increase in friction factor. The fact that there are too many parameters to be examined such as geometries of wavy channels and obstacles, arrangements of obstacles in duct, and fluid/flow properties have led to an increase in studies. The main purpose of these studies is to increase heat transfer without a significant increase in pressure loss. The studies on this subject are still ongoing. In addition, according to the open literature, no study has been found investigating the effects of different positions of circular obstacles on turbulent flow and heat transfer in a rectangular grooved channel. Therefore, the present study focuses investigating the flow and thermal characteristics in the rectangular grooved channels

with different positions of circular obstacles.

Materials and Methods

Description of Numerical Geometry

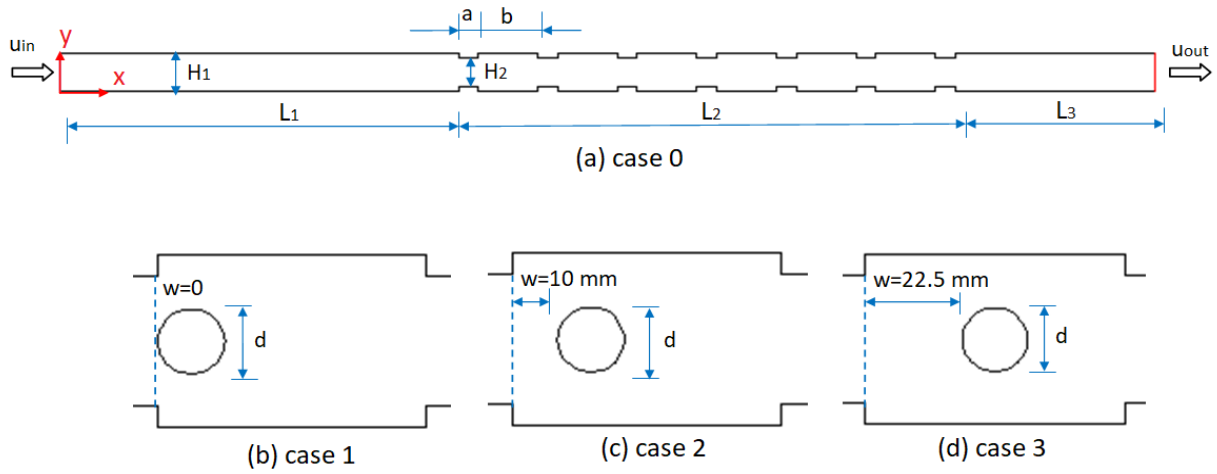

Figure 1. Geometries of the numerical model, (a) case 0, (b) case 1, (c) case 2, (d) case 3.

Figure 1 indicates 2d numerical model of rectangular grooved channels with circular obstacles in different positions. The maximum and minimum height of the channel are H_1 = 40 mm and H_2 = 30 mm, respectively. There is an adiabatic flat part of $L_1 = 10H_1$ and $L_3 = 5H_1$ at the inlet and outlet of the duct, respectively. The length of the grooved part of the duct is L_2 = 500 mm. The lengths a, and b of the rectangular corrugated parts are 20 and 60 mm, respectively. The diameters of the obstacles are d=15 mm. The channel consists of a total of 6 grooved sections. Channel flow without circular obstacles is defined as Case 0. Other channel flows are named according to the positioning of the circular obstacles in the rectangular corrugated channel and presented in Table 1.

Table 1. Descriptions of the channel flows

Channel flow	The position of the circular obstacles, (w)
Case 0	without circular obstacles
Case 1	w = 0 mm, with circular obstacles
Case 2	w = 10 mm, with circular obstacles
Case 3	w = 22.5 mm, with circular obstacles

Governing Equations

In the present study, the medium fluid is air. The fluid is considered as incompressible and Newtonian type. The fluid flows in the turbulent regime and at steady conditions. Fluid

properties are constant. Radiation and gravity effects are ignored. For these assumptions, the conservation equations are written by (Zontul et al. 2021):

$$\frac{\partial}{\partial x_i}(\rho\bar{u}_i) = 0 \tag{1}$$

$$\frac{\partial}{\partial t}(\rho\bar{u}_i) + \frac{\partial}{\partial x_j}\left(\rho\bar{u}_i\bar{u}_j\right) = -\frac{\partial\bar{p}}{\partial x_i} + \frac{\partial}{\partial x_j}\left[(\mu+\mu_t)\left(\frac{\partial\bar{u}_i}{\partial x_j}+\frac{\partial\bar{u}_j}{\partial x_i}\right)\right] - \rho\overline{u_i'u_j'} \tag{2}$$

$$\frac{\partial}{\partial t}(\rho c\bar{T}) + \frac{\partial}{\partial x_j}(\rho\bar{u}_i\bar{T}) = \frac{\partial}{\partial x_j}\left[(\Gamma+\Gamma_t)\left(\frac{\partial\bar{T}}{\partial x_j}\right)\right] \tag{3}$$

$$-\rho\overline{u_i'u_j'} = (\mu_t)\left(\frac{\partial u_i}{\partial x_j}+\frac{\partial u_j}{\partial x_i}\right) \tag{4}$$

$$\frac{\partial}{\partial t}(\rho k) + \frac{\partial}{\partial x_i}(\rho k\bar{u}_i) = \frac{\partial}{\partial x_j}\left[\left(\mu+\frac{\mu_t}{\sigma_k}\right)\frac{\partial k}{\partial x_j}\right] + G_k - \rho\varepsilon \tag{5}$$

$$\frac{\partial}{\partial t}(\rho\varepsilon) + \frac{\partial}{\partial x_i}(\rho\varepsilon\bar{u}_i) = \frac{\partial}{\partial x_j}\left[\left(\mu+\frac{\mu_t}{\sigma_\varepsilon}\right)\frac{\partial\varepsilon}{\partial x_j}\right] + C_{1\varepsilon}\frac{\varepsilon}{k}G_k - C_{2\varepsilon}\rho\frac{\varepsilon^2}{k} \tag{6}$$

In this work, the hydrodynamic and thermal behaviors in the rectangular grooved duct with different positions of the circular obstacles were studied for varying Reynolds numbers ($2000 \leq Re \leq 10000$).

Reynolds number, Re is given by (Akcay, 2023b):

$$Re = \frac{\rho u_{in} D_h}{\mu} \tag{7}$$

where D_h, u_{in}, ρ, and μ show the hydraulic diameter, the velocity of fluid, the density, and the dynamic viscosity, respectively.

The mean Nusselt number, Nu is calculated by (Akcay 2023b):

$$Nu = \frac{h\,D_h}{k} \tag{8}$$

where h is heat transfer coefficient, and k indicates thermal conductivity.

The heat transfer coefficient, h is obtained by (Akcay 2023a):

$$h = \frac{q''}{\Delta T} \tag{9}$$

where ΔT is temperature difference, and q" indicates heat flux.

The relative Nusselt number, Nu_{rel} is described as the ratio of the Nusselt number (Nu_d) in the rectangular grooved duct with obstacles to the Nusselt number (Nu_o) in the rectangular grooved duct without obstacles and is calculated as (Akcay 2023a):

$$Nu_{rel} = \frac{Nu_d}{Nu_o} \tag{10}$$

The friction factor, f is found by (Zontul et al. 2021):

$$f = \frac{2\Delta P D_h}{\rho L u_{in}^2} \tag{11}$$

The relative friction factor, f_{rel} is obtained by (Akcay 2022):

$$f_{rel} = \frac{f_d}{f_o} \quad (12)$$

where, f_o and f_d are the friction factors for grooved duct without obstacles and grooved duct with obstacles, respectively.

The thermo-hydraulic performance, THP can be computed by (Zontul et al. 2021):

$$THP = \frac{Nu_{rel}}{(f_{rel})^{1/3}} \quad (13)$$

Numerical Procedure

The numerical simulations were carried out with FLUENT software (2015). The solution domain was first divided into cells. Due to the high mesh quality (0.92), the triangular-shaped elements were preferred in the numerical model. Detail of the mesh structure for Case 3 was shown in Figure 2. The second-order upwind scheme was utilized to discretize of the convectional terms. The SIMPLE algorithm was employed for the pressure-velocity coupling. The standard k-ε turbulence model was considered as viscous model. The convergence values were set to 10^{-7} in the energy equations, 10^{-5} in other equations. As a result of the mesh independence test, it was decided that 101254 element numbers are sufficient for the calculations in the rectangular grooved duct with circular obstacle (Case 3). Nusselt numbers with grid numbers for Case 3 at Re=10000 were given in Table 2.

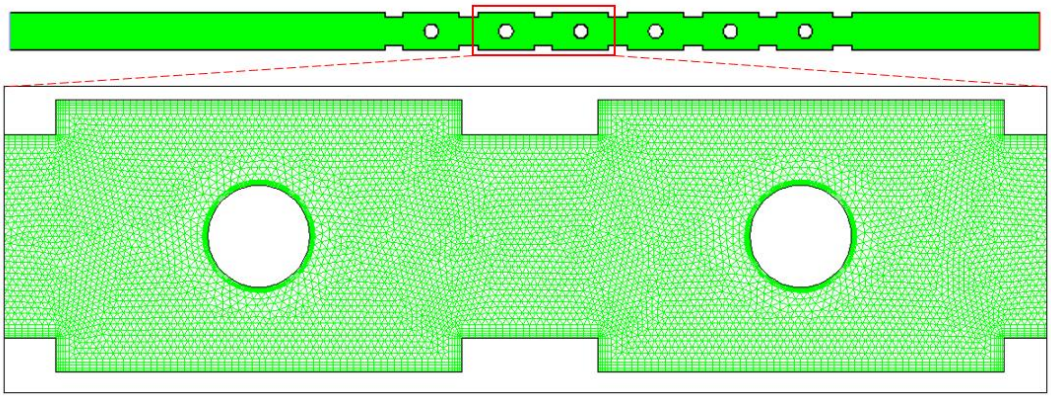

Figure 2. Mesh structure of the numerical model for Case 3.

Table 2. Grid independence testing (Case 3 and Re=10000)

Element number	Nusselt number	Difference, %
47824	10.825	-
72826	12.187	11.18
101254	13.152	7.37
134468	13.412	1.98
166542	13.524	0.83

Boundary Conditions and Validation

For the solutions, some boundary conditions were performed to the numerical model. The medium fluid enters the duct with a uniform velocity (u_{in}) and a constant temperature (T_{in} = 300 K). The pressure outlet condition was applied at the duct exit. The straight sections of the duct (L_1 and L_3) were described as adiabatic. The rectangular corrugated walls of the channel (L_2) were maintained at a constant temperature (T_w = 350 K). The obstacles have non-slip and adiabatic conditions. Moreover, the non-slip conditions were set for flat and grooved walls of the duct.

The results of this numerical study were compared to the results of Brodniansk´a and Kotˇsmíd (2023). The reference study (Brodniansk´a and Kotˇsmíd, 2023) experimentally and numerically calculated the heat transfer coefficient at the mass flow rate of 5 m^3/h for a straight duct with a height of 40 mm. In this study, a straight duct with the same hydraulic diameter as the reference study was considered and solutions were compared using similar flow conditions. The findings of this work and the results of the previous work were indicated in Figure 3.

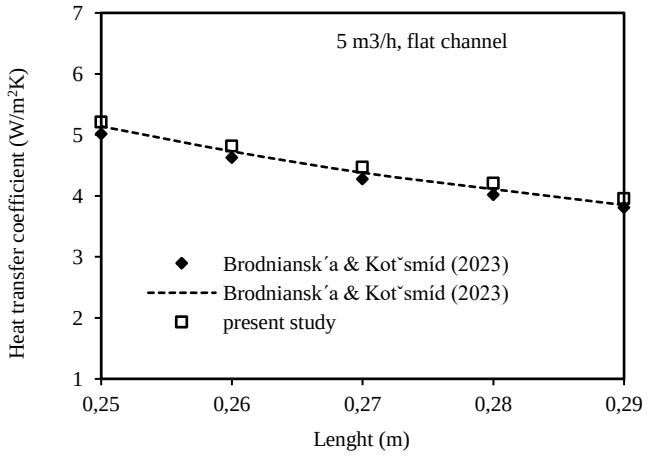

Figure 3. Validation of the numerical study.

In the numerical work, the velocity and temperature contours were obtained in the rectangular grooved channel at varying Reynolds numbers to determine the effects of circular obstacles with different positions on the flow and temperature fields. Figure 4 indicated the images of the velocity contours for all channel flows at Re = 2000 (Fig. 4a) and Re = 10000 (Fig. 4b). It was observed that the flow fields significantly varied by the channel geometry, the positions of the circular obstacles and Re. In the Case 0, it was observed that the velocity increased in the sections where the cross-sectional area narrowed.

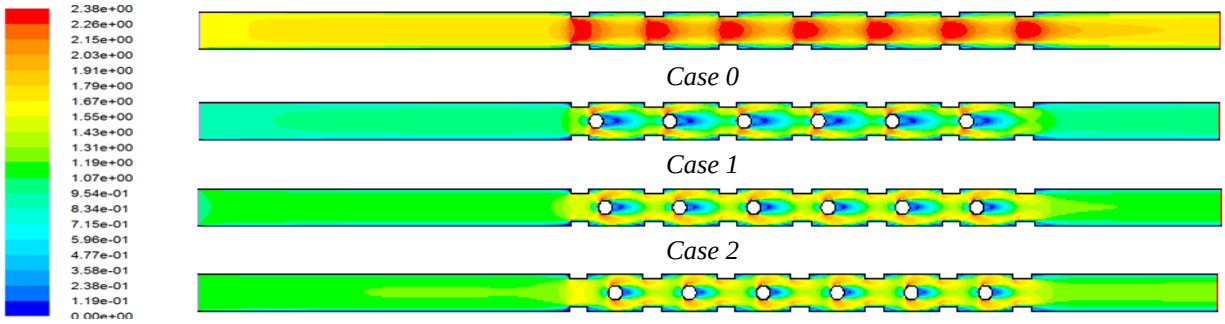

(a) Re=2000

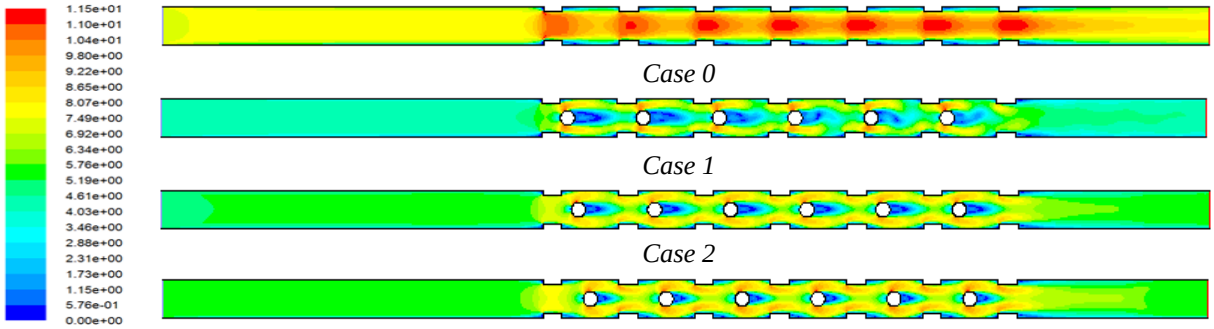

(b) Re=10000

Figure 4. The velocity contours, a-Re=2000, b- Re=10000.

The flow velocity increased in the narrowing channel sections and the primary flow was divided into two different branches due to circular obstacles. Also, the circular obstacles were directed the fluid towards the hot corrugated walls. The contact of the colder fluid with the hot corrugated walls was ensured. It was observed that the flow rejoined after each circular obstacle (Fig. 4a). As the Reynolds number increases, momentum and mass transfer in the channel increases. Thus, the hot corrugated walls were brought into contact with more cold fluid (Fig. 4b). At Case 1, it was observed that the stagnant fluid region behind the obstacles is larger than Case 3.

Figure 5 indicated the images of the temperature fields for all channel flows at Re = 2000 (Fig. 5a) and Re = 10000 (Fig. 5b). The temperature gradients in the channels were affected by the position of the circular obstacles and the Reynolds numbers. At Re = 2000, the temperature gradient is quite high in all channel flows. It was seen that the temperature gradient highly decreased at Re = 10000. Increasing Reynolds number allowed more cold fluid to contact the grooved channel surfaces. The obstacles directing the fluid to the corrugated surfaces contributed to the reduction of surface temperature of the channel.

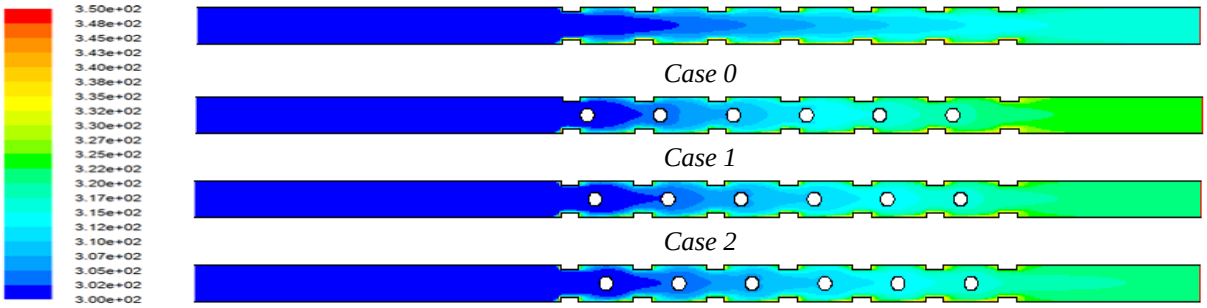

(a) Re=2000

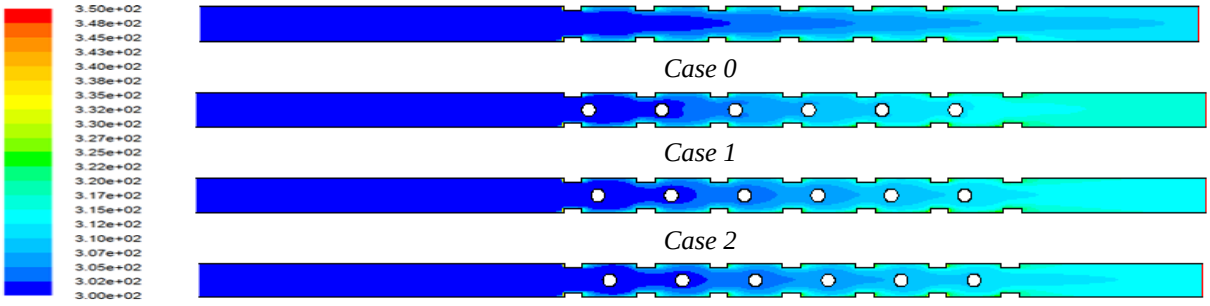

(b) Re=10000

Figure 5. Temperature contours, (a) Re=2000, (b) Re=10000

Figure 6 presented the velocity contours (a) and temperature fields (b) at Re = 8000 for all channel flows. It was understood from Figure 6a that the location of circular obstacles has a significant effect on the flow fields. Placing circular obstacles at the beginning of each corrugated cavity provides better fluid contact with the corrugated channel surfaces (Case 1). Because in Case 1, the fluid divides into two at the entrance of the corrugated cavity and moves along the corrugated surface. The shifting of circular obstacles towards the middle of the corrugated cavity delays the separation of the flow into two branches and causes the corrugated surfaces to come into less contact with the fluid (Case 3). Figure 6b indicated changes of temperature fields in the channels due to the circular obstacles. The positions of circular obstacles greatly affected the temperature structures in the channel and on the corrugated surfaces. It was observed that the minimum temperature gradient was in Case 1 and the maximum temperature gradient was in Case 0.

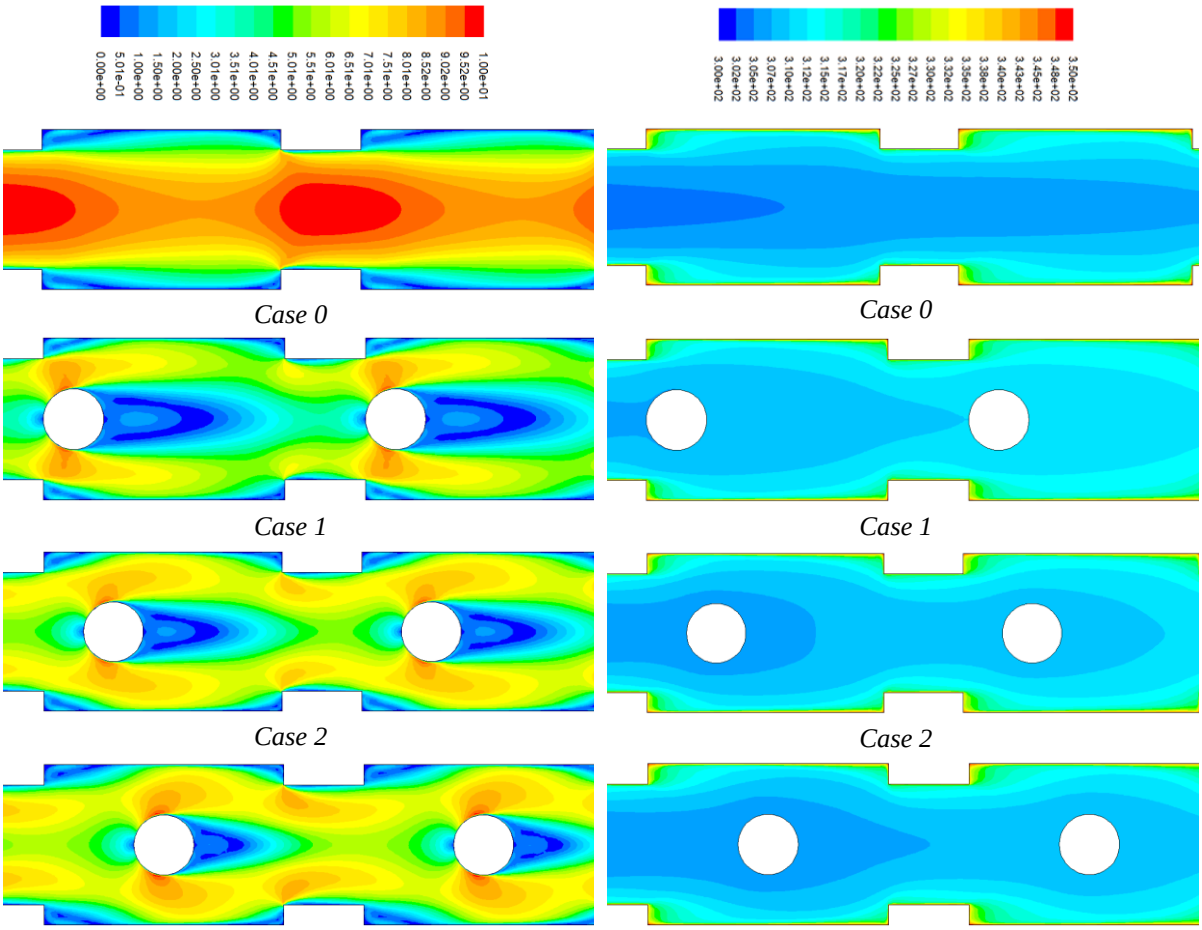

(a) Velocity contours (b) Temperature contours

Figure 6. (a) Velocity contours, (b) Temperature contours at Re=8000 for all channel configurations

Figure 7a indicates the Nusselt number versus the Reynolds number for all channel cases. The heat transfer improved with increasing Reynolds number. The all positions of the circular obstacles remarkably increased the Nusselt number compared to duct without circular obstacles (Case 0). The maximum heat transfer was obtained in the Case 1, followed by the Case 2 and Case 3, respectively. At Re = 10000, the highest heat transfer was achieved to be Nu = 16.05 in the Case 1 and the lowest Nusselt number was to be Nu = 9 in the Case 0. Figure 7b demonstrated the relative Nusselt number versus the Reynolds number. The Nusselt number obtained in the channel flow without circular obstacles (named Case 0) was accepted as a reference. The relative Nusselt number for all positions of the circular obstacles was obtained to be higher than the Case 0. However, this increment for the Case 1 is to be greater. In Case 1, heat transfer improved by 1.78 times compared to Case 0 at Re=10000.

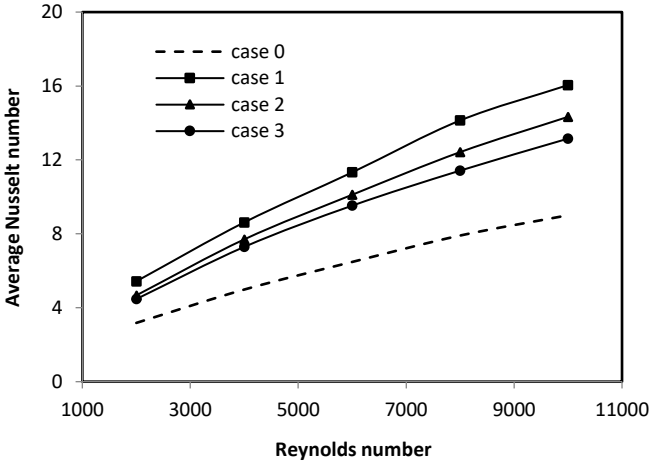

a

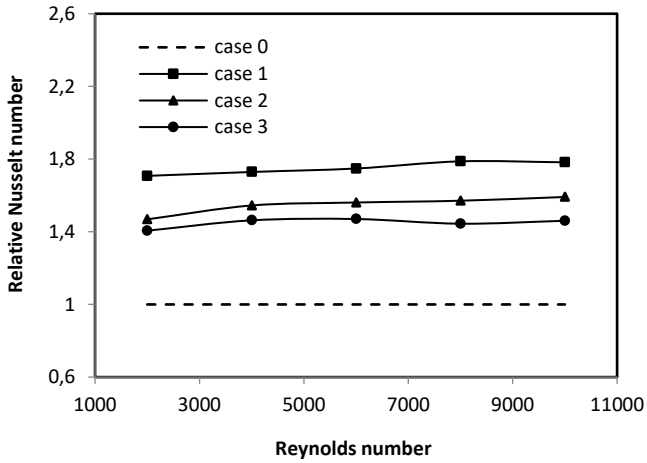

b

Figure 7. (a) Nusselt number with Re, **(b)** Relative Nusselt number with Re for all channel cases.

Figure 8a demonstrates the pressure drop with the Reynolds number for all channel configurations. The pressure drop increased with Re. Because the circular obstacles block the flow path in the channel and create resistance to flow. In Case 1, higher Nu was obtained than in other obstacle cases because the flow contacts hot surfaces better (Fig. 7a). However, Case 1 considerably blocks the flow path. Therefore, the pressure drop increased in Case 1. The shifting of circular obstacles towards the flow direction partially opens the flow path. For this reason, less pressure drop was obtained in Case 3 than in Case 1. The obstacles considerably increased the pressure drop compared to Case 0. The maximum pressure loss was found in the Case 1, followed by the Case 2 and Case 3. At Re = 10000, the highest-pressure drop was found to be 132.59 Pa in the Case 1 and the lowest pressure drop was to be 24.53 Pa in the Case 0. In Figure 8b was given the friction factor with Re in all flow cases. The friction factor diminished with Re. The friction factor of Case 3 is much less than Case 1 and Case 2. The friction factor

was found to be higher in Case 1 than in Case 2 and Case 3 due to more obstruction of the flow field. The highest average friction factor was obtained to be 0.213 in Case 1 at Re=2000.

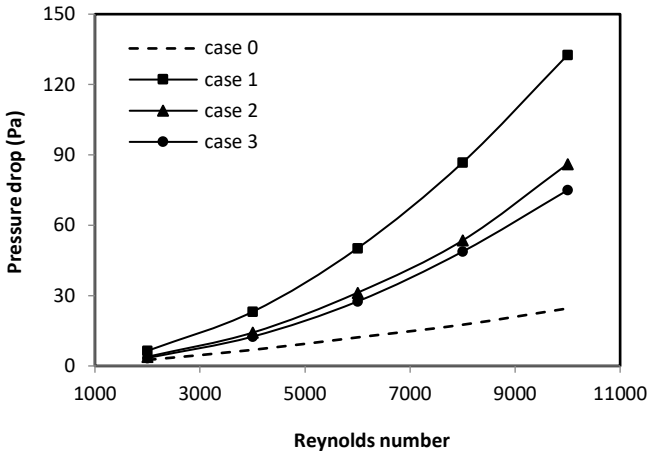

a

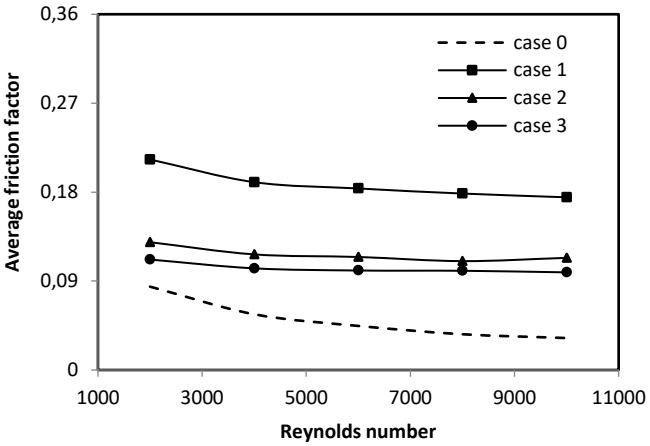

b

Figure 8. (**a)** Pressure drop versus Re, **(b)** Average friction factor versus Re.

Figure 9a indicates the relative friction factor with the Reynolds number for all flow configurations. The corrugated channel without obstacles (Case 0) is considered as reference. The relative friction factor increased with Re. The circular obstacles were increased the relative friction factor according to Case 0. The highest relative friction factor was found to be 3.93 in the Case 1 at Re = 10000. Figure 9b demonstrates the thermo-hydraulic performance (THP) versus the Re. As Re increases, the performance factor decreases. Although the obstacles increased the heat transfer, they also caused an increment in pressure loss in the duct. The best performance value was found in the Case 2. Because the pressure drop in the Case 2 is lower than the Case 1, and heat transfer in the Case 2 is higher than the Case 3. The highest THP was calculated to be 1.44 in the Case 2 and at Re = 2000.

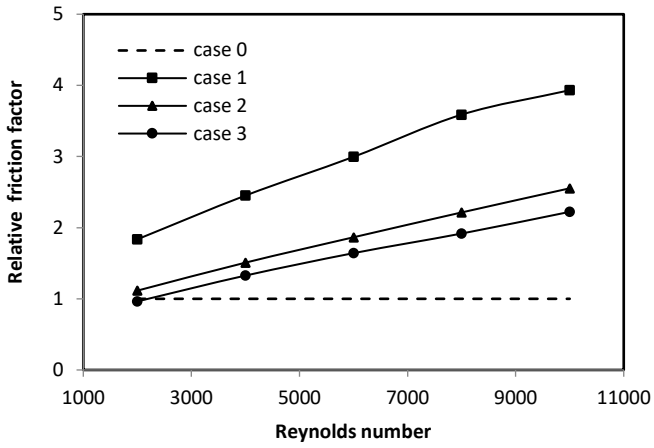

a

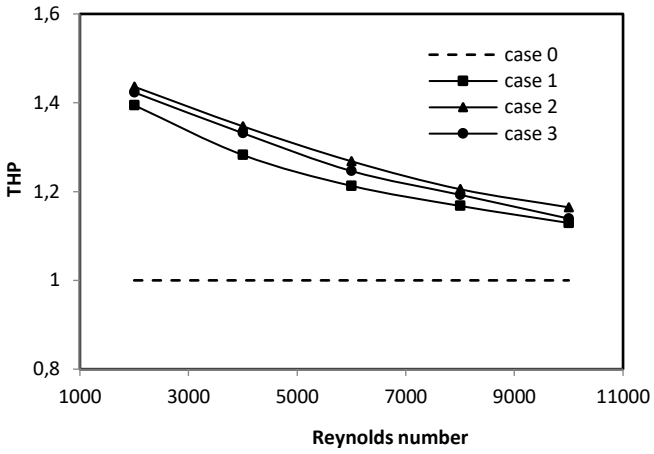

b

Figure 9. (a) Relative friction factor versus Re, **(b)** THP versus Re

Conclusion

The effects on hydraulic and thermal performance of different placements of circular obstacles in a rectangular grooved channel have not been investigated to date according to the open literature. Therefore, the work numerically evaluated the impacts of circular obstacles with three different positions on hydrodynamic and thermal performance in a rectangular grooved duct. The simulations were carried out for different Reynolds numbers ($2000 \leq Re \leq 10000$). The thermal and flow fields were obtained in the duct to observe the effects of the circular obstacles with different positions. The important findings obtained in the work were given below:

- The thermal and flow contours were significantly affected by the positions of the circular obstacles and the Reynolds numbers.
- For all flow cases, the average Nusselt number increased with the Reynolds number.

The maximum Nusselt number was obtained to be Nu = 16.05 in the Case 1 and at Re = 10000.

- The maximum relative Nu was found to be 1.78 in the Case 1 and at Re = 10000.
- For all flow cases, as the Re increased, the average friction factor diminished. The average friction factor of the Case 3 was obtained much less than Case1 and Case 2.
- In the presence of circular obstacles, the maximum pressure drop was 132.59 Pa in Case 1, while the lowest was 24.53 Pa in Case 3.
- For all channel configurations, as the Re increased, the thermo-hydraulic performance decreased. The best THP was obtained to be 1.44 in the Case 2 and at Re = 2000.

Nomenclature

D_h	hydraulic diameter (m)	ΔP	pressure difference (Pa)
d	diameter of circular obstacles (m)	u	average velocity (m/s)
f	friction factor	w	distance of circular obstacles (m)
h	heat convection coefficient (W/m^2K)		
H	channel height (m)	***Greek symbols***	
k	heat conduction coefficient (W/mK)	μ	dynamic viscosity (kg/ms)
L	channel length (m)	ρ	density of fluid (kg/m^3)
Nu	Nusselt number [hD/k]	υ	kinematic viscosity (m^2/s)
Pr	Prandtl number [$\mu C/k$]	***Subscripts***	
Re	Reynolds number (uD_h/υ)	d	circular obstacle case
T	temperature (K)	o	without circular obstacle case
THP	Thermo-hydraulic performance [$Nu_{rel}/f_{rel}^{1/3}$)	rel	relative

Researchers' Contribution Rate Declaration Summary

The author has declared that she provides its own contribution to the article.

Conflict of Interest

The author has declared that there are no competing interests.

References

Ahmed M, Yusoff M, Ng K, Shuaib N., 2014. Effect of corrugation profile on the thermal–hydraulic performance of corrugated channels using CuO–water nanofluid. Case Studies in Thermal Engineering, 4: 65-75.

Ajarostaghi SSM, Zaboli M, Javadi H, Badenes B, Urchueguia JF., 2022. A review of recent passive heat transfer enhancement methods. Energies, 15: 986.

Akcay S, Akdag U., 2023. Heat transfer enhancement in a channel with inclined baffles under pulsating flow: A CFD study. Journal of Enhanced Heat Transfer, 30(5): 61-79.

Akcay S., 2022. Numerical analysis of heat transfer improvement for pulsating flow in a periodic corrugated channel with discrete V-type winglets. International Communications in Heat Mass Transfer, 134: 105991.

Akcay S., 2023a. Heat transfer analysis of pulsating nanofluid flow in a semicircular wavy channel with baffles. Sādhanā, 48: 57.

Akcay S., 2023b. Numerical analysis of hydraulic and thermal performance of Al_2O_3-water nanofluid in a zigzag channel with central winglets. Gazi University Journal of Science, 36(1): 383-397.

Akdag U, Akcay S, Demiral D., 2014. Heat transfer enhancement with laminar pulsating nanofluid flow in a wavy channel. International Communications in Heat and Mass Transfer, 59: 17–23.

Akdag U, Akcay S, Demiral D., 2016. Heat transfer enhancement with nanofluids under laminar pulsating flow in a trapezoidal-corrugated channel. Progress in Computational Fluid Dynamics, 17(5): 302-312.

Akdag U, Akcay S, Demiral D., 2019. Heat transfer in a triangular wavy channel with CuO-water nanofluids under pulsating flow. Thermal Science, 23(1): 191-205.

Alfellag MA, Ahmed HE, Jehad MG, Farhan AA., 2022. The hydrothermal performance enhancement techniques of corrugated channels: A review. Journal of Thermal Analysis and Calorimetry, 147: 10177-10206.

Ameur H, Sahel D., 2019. Effect of some parameters on the thermo-hydraulic characteristics of a channel heat exchanger with corrugated walls. Journal of Mechanical and Energy Engineering, 3: 53-60

ANSYS Inc., 2015. ANSYS fluent user guide and theory guide- release 15.0, USA.

Bensaci CE, Moummi A, Sanchez de la Flor FJ, Rodriguez Jara EA, Rincon-Casado A, Ruiz-Pardo A., 2020. Numerical and experimental study of the heat transfer and hydraulic

performance of solar air heaters with different baffle positions. Renew Energy, 155: 1231–1244.

Brodniansk´a Z, Kotˇsmíd S., 2023. Heat transfer enhancement in the novel wavy shaped heat exchanger channel with cylindrical vortex generators. Applied Thermal Engineering, 220: 119720.

Feng CN, Liang CH, Li ZX., 2022. Friction factor and heat transfer evaluation of cross-corrugated triangular flow channels with trapezoidal baffles. Energy and Buildings, 257: 111816.

Handoyo EA, Ichsani D., 2016. Numerical studies on the effect of delta-shaped obstacles' spacing on the heat transfer and pressure drop in V-corrugated channel of solar air heater. Solar Energy, 131: 47-60.

Inan AT, Koten H, Kartal MK., 2023. Experimental comparison and CFD analysis of conventional shell and tube heat exchanger with new design geometry at different baffle intervals. Numerical Heat Transfer, Part A: Applications, 83(5): 522-533.

Krishnan EN, Ramin H, Guruabalan A., Simonson CJ., 2021. Experimental investigation on thermo-hydraulic performance of triangular cross-corrugated flow passages. International Communications in Heat and Mass Transfer, 122: 105160.

Kurtulmus N, Sahin B., 2019. A review of hydrodynamics and heat transfer through corrugated channels. International Communications in Heat and Mass Transfer, 108: 104307.

Li ZX, Sung SQ, Wang C, Liang CH, Zeng S, Zhong T, Hud WP, Feng CN., 2022. The effect of trapezoidal baffles on heat and flow characteristics of a cross-corrugated triangular duct. Case Studies in Thermal Engineering, 33: 101903.

Nfawa SR, Abu-Talib AR, Masuri SU, Basri AA, Hasini H., 2021. Heat transfer enhancement in a corrugated-trapezoidal channel using winglet vortex generators. CFD Letter, 11: 69-80.

Salami M, Khoshvaght-Aliabadi M, Feizabadi A., 2019. Investigation of corrugated channel performance with different wave shapes. Journal of Thermal Analysis and Calorimetry, 138: 3159-3174.

Selimefendigil F, Öztop HF., 2016. Numerical study of forced convection of nanofluid flow over a backward facing step with a corrugated bottom wall in the presence of different shaped obstacles. Heat Transfer Engineering, 37(15): 1280-1292.

Shahsavar SS, Alimohammadi I, Askari B, Ali HM., 2021. Numerical investigation of the effect of corrugation profile on the hydrothermal characteristics and entropy generation

behavior of laminar forced convection of non-Newtonian water/CMC-CuO nanofluid flow inside a wavy channel. International Communications in Heat and Mass Transfer, 121: 105117.

Togun H, Homod RZ, Yaseen ZM, Abed AM, Dhabab JM, Ibrahem RK, Dhahbi S, Rashidi MM, Ahmadi G, Yaïci W, Mahdi JM., 2022. Efficient heat transfer augmentation in channels with semicircle ribs and hybrid Al_2O_3-Cu/water nanofluids. Nanomaterials, 12(15): 2720.

Zhang L, Che D., 2011. Turbulence models for fluid flow and heat transfer between cross corrugated plates. Numerical Heat Transfer, Part A: Applications, 60: 410-440.

Zontul H, Hamzah H, Kurtulmuş N, Şahin B., 2021. Investigation of convective heat transfer and flow hydrodynamics in rectangular grooved channels. International Communications in Heat and Mass Transfer, 126: 105366.